



HAL
open science

Linear tubular switched reluctance motor for heart assistance circulatory

Jean-François Llibre, N. Martinez, Bertrand Nogarède, P. Leprince

► **To cite this version:**

Jean-François Llibre, N. Martinez, Bertrand Nogarède, P. Leprince. Linear tubular switched reluctance motor for heart assistance circulatory. 2011 10th International Workshop on Electronics, Control, Measurement and Signals (ECMS), Jun 2011, Liberec, Czech Republic. 6 p., 10.1109/IWECMS.2011.5952367 . hal-03558810

HAL Id: hal-03558810

<https://ut3-toulouseinp.hal.science/hal-03558810v1>

Submitted on 4 Feb 2022

HAL is a multi-disciplinary open access archive for the deposit and dissemination of scientific research documents, whether they are published or not. The documents may come from teaching and research institutions in France or abroad, or from public or private research centers.

L'archive ouverte pluridisciplinaire **HAL**, est destinée au dépôt et à la diffusion de documents scientifiques de niveau recherche, publiés ou non, émanant des établissements d'enseignement et de recherche français ou étrangers, des laboratoires publics ou privés.

Linear tubular switched reluctance motor for heart assistance circulatory

Analytical and finite element modeling

J-F. Llibre, N. Martinez, B. Nogarède

Université de Toulouse; INPT, UPS; ENSEEIHT
CNRS; LAPLACE;
2 rue Charles Camichel, BP7122
F-31071, Toulouse Cedex 7, France
llibre@laplace.univ-tlse.fr

P. Leprince

Institut de Cardiologie
Groupe Hospitalier Pitié-Salpêtrière
47-83 Boulevard de l'hôpital
F-75013, Paris, France

Abstract—A linear tubular switched reluctance motor is presented. This actuator is devoted to be used as a left ventricular assist device (LVAD). In order to avoid thrombosis, this actuator includes pump and valve functions. By using a St. Jude Medical mechanical valve inside the tubular mover, a pulsatile flow is created in the descending aorta. A linear model of a basic pattern of the actuator based on a reluctance network is developed. Then, a two dimensions finite element method analysis is performed in order to check the analytically calculated performances. Relying on these both models, specific requirements for the design of this kind of motor are discussed.

Keywords - switched reluctance motor; finite element; tubular mover; heart assistance

I. INTRODUCTION

Patients suffering from severe heart failure require mechanical circulatory support (MCS). Most of the time, a left ventricular assist device (LVAD) is used. This last one assists the failing left ventricle by providing an additional flow of blood in the body.

At the beginning of heart transplantation, MCSs were pneumatic providing a pulsatile flow. Thus the MCS functioning was close to the heart functioning. The major limitations were the pump bulk, the limited mobility because of a large drive console and the need for chronic anticoagulation [1]. Actually, the last generation of MCS is electromagnetic and provides a continuous flow. For example, the “Debakey VAD”, the “Hearmate II” and the “Jarvik 2000” are miniaturized axial flow pumps (with a turbine and a motor) [2]. The success of these devices is limited by the risk of thrombus in the pump. Moreover, the impact of continuous blood flow on the body remains unknown for the scientific and medical community [3].

We proposed here a new LVAD concept of pulsatile blood pump to be implanted in the aorta descending which is an evolution of that presented in [4]. In order to avoid thrombotic events, this pump called “Pulsamag” incorporates the valve and pump functions. The actuator is a linear switched reluctance motor (LSRM). The stator and the mover have a cylindrical or

tubular shape. A mechanical unidirectional valve is placed inside the mover. The topology of the motor and its main characteristics are described in section II. Section III gives some considerations on the dimensioning and particularly the thrust calculated analytically with the help of a basic pattern of the actuator. A linear model based on a reluctance network of the basic pattern is presented in section IV, while section V is dedicated to the results obtained via a two dimensions finite element method (2D-FEM) analysis. Finally, section VI describes the conclusion and perspectives of the work.

II. PULSATILE PUMP CONCEPT DESCRIPTION

A. Overview of switched reluctance motors

For the application considered, the LSRM is a good candidate. Indeed, its structure is simple and robust. One characteristic is the lack of windings on either the stator or mover part. Usually, the windings are concentrated around the poles rather than distributed. So, the manufacturing and the maintenance are easier and a functioning with a phase shorted or open is possible [5, 6].

There are several types of LSRM. The most frequently studied are counterparts of rotary switched reluctance motors (RSRMs) [5, 6, 7, 8]. The linear configuration can be obtained from the rotating configuration by cutting radially and by unrolling. The windings are concentrated around the poles and the static part is a plate. In [9], a configuration with two E-cores mounted on a carrier structure that moves along a stationary bar is investigated (two air gaps). In [10], a structure called transverse flux tubular switched reluctance motor (TSRM) with concentrated windings around the stator poles is studied (the stator is similar to RSRM one).

An interesting structure is the cylindrical LSRM [11, 12, 13, 14] where the mover part has no windings like [10]. It consists of a moving ferromagnetic cylinder with transverse slots and an outer cylindrical stator containing a number of identical phase sets. Each set consists of a magnetic core, formed of two discs and a ring, and an enclosed solenoidal winding. In the same manner, a six phase cylindrical LSRM has been developed for heart assistance circulatory [15]. A

hybrid form with permanent magnets in the stator was investigated in [16]. The linear pulse motor (LPM) designed consists of a pair of primary stators placed above and below a flat secondary mover (pancake design). A pulsatile total artificial heart (TAH) is then constituted of the LPM, two pusher plates, two sac type blood pumps and four Jellyfish valves [17]. The TAH pumps the blood by expanding and compressing the sacs according to the reciprocating motion of the pusher plates attached to the mover.

B. Presentation of our concept

The objective of the actuator to be implanted in the aorta is to provide a physiological pulsatile flow. It is planned that the actuator ensures both valve and pump functions in a small space. Our LVAD is then composed of a linear actuator (cylindrical LSRM type) equipped with a St. Jude Medical mechanical valve (unidirectional) inside the tubular mover. This 25 mm diameter valve, shown in Fig. 1, allows the blood moving.



Figure 1. St. Jude Medical mechanical valve

The actuator proposed is of the same type as the one studied by [11, 14] and is composed of eight stator coils (four phases with two coils per phase) and a tubular mover. The longitudinal cross-sectional view of “Pulsamag” is shown in Fig. 2 and a three dimensional view is shown in Fig. 3.

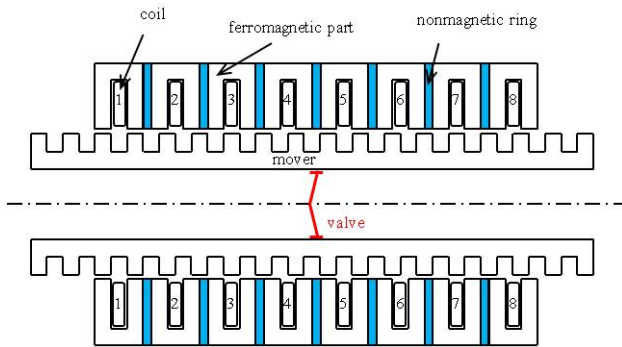


Figure 2. Basic structure of “Pulsamag”

When the phases are excited sequentially with unipolar current, a magnetic field that slides alternately from one to the other end of the actuator is generated. Then the ferromagnetic cylinder moves back and forth in order to align its saliencies with that of the excited stator phases (maximization of the magnetic flux). During the motion of the cylinder in one direction, the mechanical valve closes and pushes the fluid (blood). In the other direction, the valve opens and thus limits its influence on the fluid.

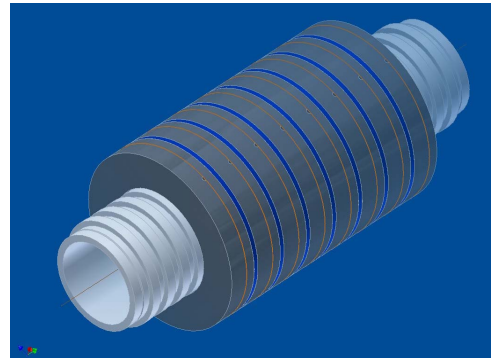


Figure 3. Three dimensional view of “Pulsamag”

In this low speed application, because of low eddy current losses, the magnetic core does not have to be made of laminated steel. Moreover, due to the cylindrical shape, the normal forces are neutralized. The other advantages of this type of actuator are its reliability, its simplicity of implementation, its ability to generate a linear motion directly (without mechanical processing)...

One of the main drawbacks is the difficulty of guiding the mover part in order to ensure a constant air gap. The latter is usually small to ensure good performances.

C. Desired mechanical characteristics

The physiological requirements for a LVAD are a flow of 3 liters per minute (l/min) and a pressure of 120 mmHg (16 kPa) under a 2 Hz frequency (120 beats per minute). The thrust F (in N) and the stroke L (in mm) of the mover are given by:

$$L = \frac{10^3}{6} \frac{Q}{S \cdot f} \quad F = \frac{P \cdot S}{10} \quad (1)$$

Where Q is the flow (l/min), S is the cross-section (cm²), f is the frequency (Hz) and P is the pressure (kPa).

Thus, with a 25 mm diameter valve, the stroke and the required thrust could reach 51 mm and 8 N respectively. In the next section, we present an analytical model based on a basic pattern in order to give elements on the dimensioning of the actuator.

III. ANALYTICAL MODEL OF THE ACTUATOR

A. Basic pattern

We can see in Fig. 2 that each phase set of the actuator forms an independent magnetic circuit thanks to the nonmagnetic ring. So we can consider one set and extrapolate the results to the entire actuator.

The basic pattern of the actuator is then constituted of a stator ferromagnetic part with one slot (with a coil) and two teeth and a mover ferromagnetic part with one slot (without coil) and two teeth as we can see in Fig. 4. To build the whole actuator, the modules are stacked, separated by a stator nonmagnetic ring.

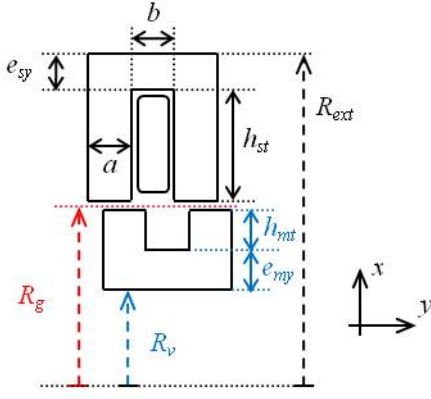


Figure 4. Basic pattern

The notations of the axial and radial geometrical dimensions, presented in Fig. 4 are: a tooth width, b slot width, R_v valve radius, R_g air gap radius, R_{ext} external radius, h_{mt} mover tooth length, e_{my} mover yoke thickness, h_{st} stator tooth length and e_{sy} stator yoke thickness.

In order to ensure a smooth and regular functioning, we have chosen the tooth pitch of the stator λ_s and the tooth pitch of the mover λ_m equal:

$$\lambda_s = \lambda_m = \lambda = a + b. \quad (2)$$

The tooth width a and the slot width b of the stator and the mover are chosen equal too:

$$a = b. \quad (3)$$

B. Analytical static force calculation

When operating in linear mode, the magnetic energy W_{mag} and the magnetic co-energy W_c are equal and can be expressed by:

$$W_{mag}(i, y) = W_c(i, y) = \frac{1}{2} \mathcal{P}(y) (Ni)^2. \quad (4)$$

Where N is the number of coil turns, i is the current supply, y is the position of the mover and \mathcal{P} is the permeance. The force F_y along axis y is done by:

$$F_y = \frac{\partial W_c(i, y)}{\partial y} \Big|_{Ni=cte} = \frac{1}{2} \frac{\partial \mathcal{P}(y)}{\partial y} (Ni)^2 \Big|_{Ni=cte}. \quad (5)$$

Assuming that the magnetic material does not saturate and that the magnetic relative permeability is infinite, the permeance \mathcal{P} in (5) is limited to the air gap permeance \mathcal{P}_g .

For a step Δy , as we can see in Fig. 5, the variation of the air gap permeance $\Delta \mathcal{P}_g$ is done by:

$$\Delta \mathcal{P}_g(y) = \frac{\mu_0 \cdot S_g}{2g} = \frac{\mu_0 \cdot (2\pi R_g \cdot \Delta y)}{2g}, \quad (6)$$

where g is the air gap length and S_g is the average cross section of the flux tube.

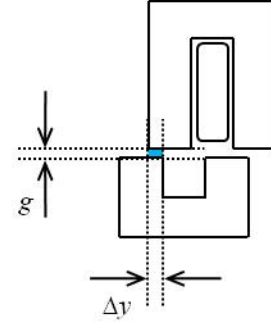


Figure 5. Calculation of air gap permeance

Finally, the mean static force for a basic pattern F_y is done by:

$$F_y = \frac{\mu_0 \pi R_g}{2g} \cdot (Ni)^2. \quad (7)$$

This expression is identical to that given by [14].

The magnetomotive force Ni can be calculated in terms of the air gap induction B_g as:

$$Ni = 2g \frac{B_g}{\mu_0}. \quad (8)$$

Then the force F_y in terms of the air gap induction B_g is:

$$F_y = \frac{2\pi}{\mu_0} \cdot g R_g B_g^2. \quad (9)$$

The same expression of the force can be found in [5, 10]:

$$F_y = \frac{B_g^2}{2\mu_0} \cdot XZ, \quad (10)$$

where X and Z are respectively equal to $2g$ and $2\pi R_g$ (the product XZ is the air gap exchange area).

C. Elements for dimensionning

According to (7), we can notice that the mean thrust is high if the air gap length g is small and the radius air gap R_g is high. In our structure, R_g is greater than the valve radius R_v but cannot be too high because of the limited volume of the actuator (implantation in the human body).

We can also notice that the thrust is proportional to the square of the magnetomotive force. Thus the increasing of the current leads to an increasing of the thrust but also an increasing of the copper loss (square increasing). One dimensioning factor for switched reluctance motors is the maximization of the mean torque per copper loss. In [14], this optimization gives the following result:

$$R_g \cong (\sqrt{2} - 1) \cdot (R_{ext} - e_{sy}). \quad (11)$$

If we neglect in (11) the stator yoke thickness e_{sy} compared to the external radius R_{ext} , the optimum ratio is 0.4 between the

air gap radius R_g and the external radius R_{ext} . Then the stator tooth length h_{st} is equal to 1.4 times R_g .

The stroke of the actuator is another major consideration for the dimensioning. To increase the stroke, we can increase the basic pattern number i.e. the phase number m and/or the coil per phase number n . By supplying several coil in serial ($n \neq 1$), both the stroke and the thrust increase.

We can notice in Fig. 2 that to separate two basic patterns, a nonmagnetic ring thickness of c value has to be inserted. The mechanical step y_p of the actuator is done by:

$$\lambda_p = \frac{\lambda}{m} = |b - c|. \quad (12)$$

For example, when the phase number one is excited, a force is produced between the stator and the mover in order to maximize the magnetic flux (stator and mover teeth in aligned position). Then the distance between the stator tooth of the next phase (phase number two for example) and the closest mover tooth is λ_p .

D. Dimensions of the prototype

The actuator presented in Fig. 2 has got $m = 4$ phases and $n = 2$ coils per phase. Moreover, the tooth and slot widths are equal as written in (3). From (12), we can deduce that:

$$\lambda_p = \frac{\lambda}{4} = \frac{a}{2} = c. \quad (13)$$

The supplying of the coils 1-5 (phase 1), 2-6 (phase 2), 3-7 (phase 3) and 4-8 (phase 4) by a four-phase current system leads to a leftward shift whereas the reverse sequence 1-5, 4-8, 3-7 and 2-6 leads to a rightward shift.

The external radius R_{ext} according to (11) will be larger than 31 mm considering the radius valve value R_v , which is equal to 12.5 mm. In order to limit the bulk of the actuator (external radius inferior to 30 mm) and the mass of the mover, we have chosen the dimensions given in Table I.

TABLE I. PROTOTYPE DIMENSIONS

Name	Abbreviation	Size (mm)
Valve radius	R_v	12.5
Mover yoke thickness	e_{my}	2
Mover tooth length	h_{mt}	1.5
Air gap	g	0.2
Air gap radius	R_g	16.1
Stator tooth length	h_{st}	9
Stator yoke thickness	e_{sy}	1.5
External radius	R_{ext}	26.7
Tooth width	a	2.9
Slot width	b	2.9
Nonmagnetic ring thickness	c	1.45

The total length of the stator L_{sT} is given by:

$$L_{sT} = m \cdot n \cdot (2a + b) + (m \cdot n - 1) \cdot c. \quad (14)$$

The total length of the mover L_{mT} is dependant of the desired stroke:

$$L_{mT} \geq stroke + L_{sT}. \quad (15)$$

With the previous dimensions done, the external length dimensions of the prototype are: $L_{sT} \cong 80$ mm and $L_{mT} \geq 130$ mm.

The total expected thrust F_{yT} is given by:

$$F_{yT} = n \cdot \frac{\mu_0 \pi R_g}{2g} \cdot (Ni)^2. \quad (16)$$

To reach the desired thrust of 8 N, the magnetomotive force Ni is equal to 158 At (considering a slot fill factor of 100 % and $n = 2$ coils per phase).

IV. LINEAR MODEL BASED ON RELUCTANCE NETWORK

A. Reluctance network

The basic pattern of Fig. 4 can be modeling by using the reluctance network of Fig. 6 [14]. We consider that the magnetic material is linear with a constant permeability μ .

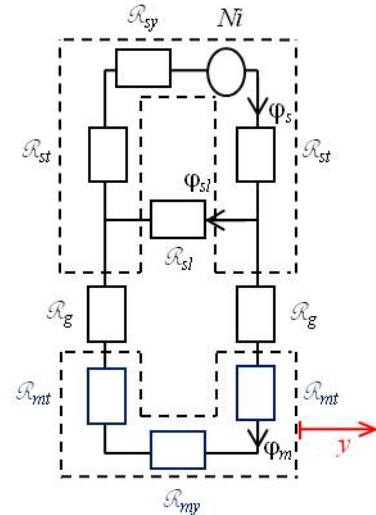


Figure 6. Reluctance network of the basic pattern

The stator flux ϕ_s is divided in one slot leakage flux ϕ_{sl} and one useful flux ϕ_m reaching the mover.

The air gap reluctance R_g varies with the position y of the mover. An axial magnetic flux flows through the stator tooth reluctance R_{st} , the mover tooth reluctance R_{mt} and the air gap reluctance R_g . A radial magnetic flux flows through the stator yoke reluctance R_{sy} and the mover yoke reluctance R_{my} . The slot leakage flux ϕ_{sl} is modeled by the specific reluctance R_{sl} .

The reluctances are listed in Table II.

TABLE II. RELUCTANCE VALUES

Name	Expression
air gap reluctance	$\mathcal{R}_g = \frac{g}{\mu_0 \cdot 2\pi R_g \Delta y}$
stator tooth reluctance	$\mathcal{R}_{st} = \frac{h_{st}}{\mu \cdot \pi [(R_{ext} - e_{sy}) + (R_g + 0.5g)] \cdot a}$
mover tooth reluctance	$\mathcal{R}_{mt} = \frac{h_{mt}}{\mu \cdot \pi [(R_g - 0.5g) + (R_g - 0.5g - h_{mt})] \cdot a}$
stator yoke reluctance	$\mathcal{R}_{sy} = \frac{2a + b}{\mu \cdot \pi [R_{ext}^2 - (R_{ext} - e_{sy})^2]}$
mover yoke reluctance	$\mathcal{R}_{my} = \frac{2a + b}{\mu \cdot \pi [(R_g - 0.5g)^2 - (R_g - 0.5g - e_{my})^2]}$
slot leakage reluctance	$\mathcal{R}_{sl} = \frac{6b}{\mu_0 \cdot \pi h_{st} (3h_{st} + 4(R_g + 0.5g))}$

B. Force calculation

With the help of Matlab software we have calculated the reluctances and the fluxes above mentioned for several magnetomotive forces in function of the displacement Δy of the mover. The relative permeability of the magnetic material was taken constant and equal to 1000.

The static force F_y for a specific value of magnetomotive force NI is done by:

$$F_{y|NI} = \frac{\Delta W_c(y)}{\Delta y} \Big|_{NI} = \frac{1}{2} NI \frac{\phi(y_k) - \phi(y_{k-1})}{y_k - y_{k-1}}. \quad (17)$$

We consider in this section that the entire slot is filled with copper (slot fill factor of 100 %) i.e.:

$$NI = bh_{st} \cdot J. \quad (18)$$

So for a current density J of 10 A/mm² in the slot, the magnetomotive force NI is equal to 261 At (26.1 mm² slot area).

By using (17), we can then calculate the force for different positions of the mover for a given magnetomotive force value. Fig. 7 shows the static force versus the relative displacement called “shift” (expressed in %) for different magnetomotive forces (the corresponding density current in the slot is between 2 A/mm² to 10 A/mm² with a step of 2 A/mm²). When the stator and the mover teeth are in aligned position (maximum flux), the shift is 0%. For a displacement equal to the mechanical step y_p , the shift is 50%.

We can notice that for a magnetomotive force of 261 At and a shift of 50 % (corresponding to the maximum thrust in the actuator), the force is near 10 N.

We can compare this result to 10.8 N which is the value obtained by using (7).

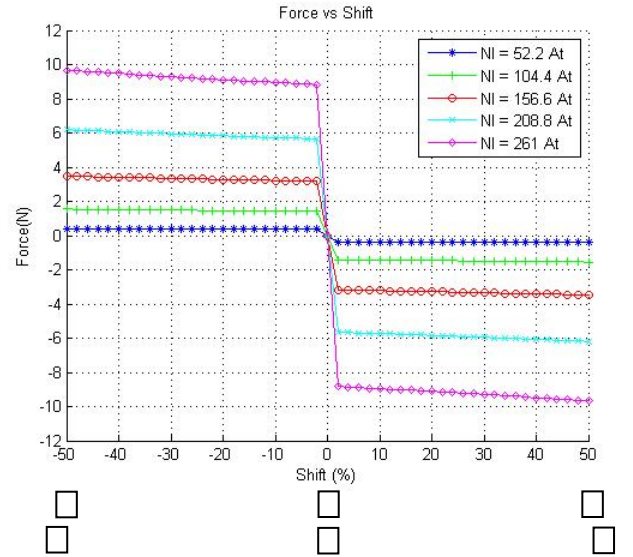
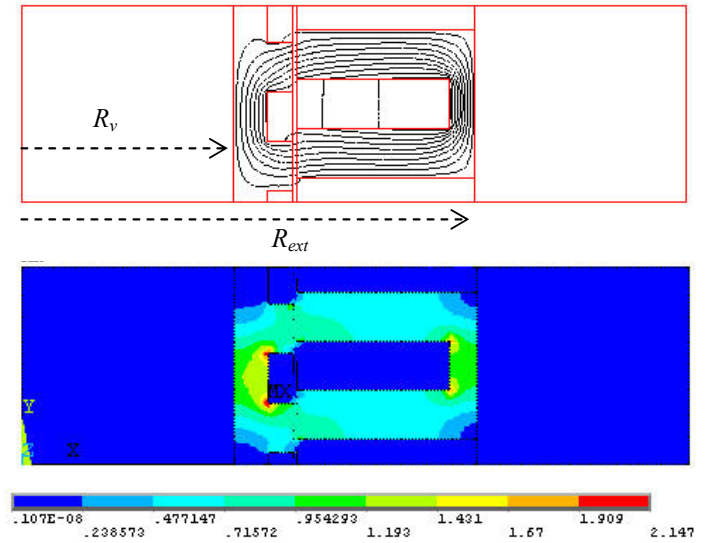


Figure 7. Force versus shift

V. TWO DIMENSION FINITE ELEMENT METHOD ANALYSIS

A. Flux density and force determination

The basic pattern of Fig. 4 has been simulated with the help of Ansys software by using the same magnetic characteristics than the previous model. We can see in Fig. 8 the flux lines and the magnetic flux density for a shift equal to 25 % and a current density in the slot equal to 10 A/mm².


 Figure 8. Flux line and magnetic flux density plots for $J = 10$ A/mm² and $shift = 25\%$

We can see that the magnetic flux density in the air gap is around 0.8 T and the induction in the yoke is around 1 T. There are some local areas where the magnetic flux density is high.

Fig. 9 shows the static electromagnetic force computed using two techniques: the Maxwell stress tensor “ F_{mx} ” and the

virtual work principle “ F_{vw} ”. We have also plotted the analytical force “ F_{th} ” calculated previously in Fig. 7.

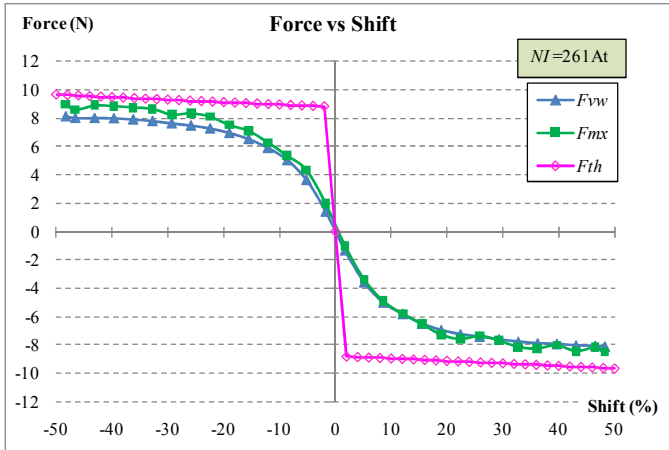


Figure 9. Force versus shift for $J = 10 \text{ A/mm}^2$ (i.e. $NI = 261 \text{ At}$)

We can notice that the forces are similar, which validates the previous model.

B. Prototype dimensioning

The prototype build is shown in Fig. 10. The active stator length is 80 mm and the mover length is 140 mm (30 mm stroke on each side) according to (14) and (15).

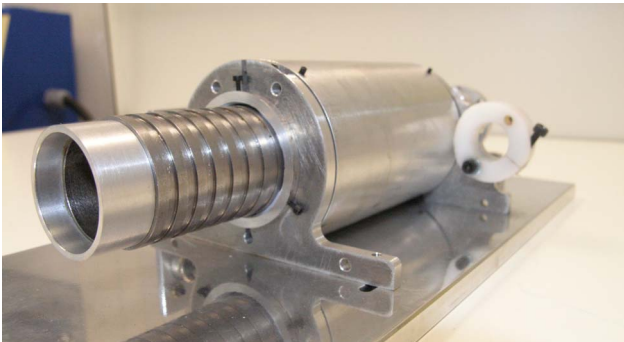


Figure 10. Pulsamag prototype

The slot fill factor is equal to 52 % and the number of turns N in a coil is equal to 155. With a supply current I equal to 1 A, the magnetomotive force is equal to 155 At and the current density in the coil is equal to 11.4 A/mm^2 .

For one basic pattern, as we can see in Fig. 7, the expected thrust will be close to 3.5 N. Because there are two coils per phase excited, the expected thrust will be equal to 7 N. In order to reach the desired thrust mentioned in II.C, it will be necessary to supply two phases at the same time or to double the current during a part of the electrical period.

VI. CONCLUSION

We have presented in this paper a linear tubular switched reluctance motor for mechanical circulatory support. A

mechanical valve is inserted inside the mover in order to create a pulsatile flow. A theoretical study and a FEM Analysis were performed on a basic pattern using linear magnetic materials. These studies suggest that the actuator can provide the stroke and the thrust necessary for the intended application. In order to validate this concept, we plan to make experimental tests for different electrical power supply strategies.

REFERENCES

- [1] P.L. DiGiorgi, Y. Naka, M.C. Oz, “Left ventricular assist devices,” Contemporary Cardiology: Surgical management of congestive heart failure, Chapter 7, 2005, pp. 155–189.
- [2] A. Blitz, J.C. Fang, “Ventricular assist devices and total artificial hearts,” Contemporary Cardiology: Device Therapy in Heart Failure, Chapter 13, 2009, pp. 339–371.
- [3] G.S. Allen, K.D. Murray, D.B. Olsen, “The importance of pulsatile and non pulsatile flow in the design of blood pumps,” Artificial Organs, vol. 21, issue 8, 1997, pp. 922–928.
- [4] N. Martinez, P. Leprince, B. Nogarede, “A novel concept of pulsatile magnetoactive pump for medical circulatory support,” 18th International Conference on Electrical Machines, ICEM, 2008, pp. 1–6.
- [5] B-S. Lee, H-K. Bae, P. Vijayaraghavan, R. Krishnan, “Design of a linear switched reluctance machine,” IEEE Trans. Ind. Appl., Vol. 36, No. 6, 2000, pp. 1571–1580.
- [6] M.R.A. Calado, A. Espirito Santo, S.J.P.S. Mariano, C.M.P. Cabrita, “Characterization of a new linear switched reluctance actuator,” International Conference on Power Engineering Energy and Electrical Drives, POWERENG’09, 2009, pp. 315–320.
- [7] D.S.B. Fonseca, C.P. Cabrita, M.R.A. Calado, “Linear switched reluctance motor. A new design methodology based on performance evaluation,” International Conference on Industrial Technology, IEEE ICIT’04, Vol. 1, 2004, pp. 519–524.
- [8] D.S.B. Fonseca, T.J.B. Godinho, C.P. Cabrita, “Electromagnetic characterization of a linear reluctance actuator. A new approach,” 18th International Conference on Electrical Machines, ICEM, 2008, pp. 1–6.
- [9] D.G. Taylor, R. Ahmed, “Current limited optimal excitation of magnetically coupled linear variable reluctance motors,” IEEE International Electric Machines and Drives Conference, IEMDC’03, Vol. 2, 2003, pp. 857–860.
- [10] I-A. Viorel, K. Hameyer, L. Strete, “Transverse flux tubular switched reluctance motor,” 11th International Conference on Optimization of Electrical and Electronic Equipment, OPTIM’08, 2008, pp. 131–136.
- [11] J. Corda, E. Skopljak, “Linear switched reluctance actuator,” 6th International Conference on Electrical Machines and Drives, 1993, pp. 535–539.
- [12] J. Corda, M. Wilkinson, “Modelling of static thrust characteristics of cylindrical linear switched reluctance actuator,” 7th International Conference on Electrical Machines and Drives, 1995, pp. 354–358.
- [13] J. Corda, B. Ouhab, “Electromagnetic design optimisation of a linear-cylindrical variable-reluctance motor,” 9th International Conference on Electrical Machines and Drives, 1999, pp. 276–280.
- [14] L. El Amraoui, F. Gillon, S. Vivier, P. Brochet, M. Benrejeb, “Optimal design approach for linear tubular machines,” IEEE International Conference on Systems Man and Cybernetics, Vol. 5, 2002, pp. 1–6.
- [15] H. Yamada, T. Hamajima, S. Xiang, N. Nishizawa, “Six-phase linear pulse motor as linear oscillatory actuator,” IEEE Trans. On Magn., Vol. MAG-23, No. 5, 1987, pp. 2841–2843.
- [16] M. Karita, Y. Sato, H. Yamada, “Mock circulatory test of linear pulse motor-driven artificial heart,” IEEE Translation Journal on Magnetism in Japan, Vol. 6, Issue 7, 1991, pp. 560–568.
- [17] H. Yamada, T. Mizuno, H. Wakiwaka, Y. Izumi, Y. Kataoka, M. Karita, M. Maeda, Y. Kikuchi, “Drive control of linear pulse motor for artificial heart,” International Conference on Power Electronic Drives and Energy Systems for Industrial Growth, Vol. 1, 1998, pp. 427–431.